Journal of Engineering Mathematics **45:** 283–308, 2003.

Surface-tension-driven flow on a moving curved surface

P.D. HOWELL
Mathematical Institute, University of Oxford, 24-29 St Giles', Oxford OX1 3LB, UK
(e-mail: howell@maths.ox.ac.uk)

Received 25 April 2002; accepted in revised form 9 September 2002

Abstract. The leading-order equations governing the flow of a thin viscous film over a moving curved substrate are derived using lubrication theory. Three possible distinguished limits are identified. In the first, the substrate is nearly flat and its curvature enters the lubrication equation for the film thickness as a body force. In the second, the substrate curvature is constant but an order of magnitude larger; this introduces an extra destabilising term to the equation. In the final regime, the radius of curvature of the substrate is comparable to the lengthscale of the film. The leading-order evolution equation for the thin film is then hyperbolic, and hence can be solved using the method of characteristics. The solution can develop finite-time singularities, which are regularised by surface tension over a short lengthscale. General inner solutions are found for the neighbourhoods of such singularities and matched with the solution of the outer hyperbolic problem. The theory is applied to two special cases: flow over a torus, which is the prototype for flow over a general curved tube, and flow on the inside of a flexible axisymmetric tube, a regime of interest in modelling pulmonary airways.

Key words: asymptotic expansions, surface tension, thin liquid films

1. Introduction

The surface-tension-driven flow of a thin liquid film over a solid substrate is of fundamental importance in many diverse applications. Examples include industrial coating flows [1, 2], the levelling of paint films [3] and biological systems such as the flow of the tear film on an eye [4] or the liquid lining of an airway [5]. Since these films are thin, mathematical models are often based on the lubrication approximation. This typically results in a single degenerate nonlinear fourth-order parabolic equation for the film thickness; see the review articles by Oron *et al.* [6] and by Myers [7].

In many processes, the substrate to be coated is not flat, and the ability of the fluid to cover and/or conform to a curved substrate is particularly of interest. Stillwagon and Larson [8] showed that a small substrate topography may be incorporated as a forcing term, proportional to the gradient of the substrate curvature, in the standard Landau-Levich equation. Stillwagon and Larson [9] included a centrifugal body force to model the flow over an uneven substrate during spin coating. Considering an isolated substrate 'feature', they decomposed the flow into an outer region, where the film is nearly flat and driven solely by centrifugal effects, and an inner quasi-static region near the feature, where surface tension becomes important. Using Stillwagon and Larson's model, Kalliadasis *et al.* [10] showed that, in steady flow, a capillary ridge forms upstream of any isolated step-like feature.

All these models are based on the lubrication approximation, essentially assuming that the slopes of the free surface and of the substrate are small, although this assumption is clearly violated by the steep substrate features considered. Mazouchi and Homsy [11] analysed the problem considered in [10] by solving the full Stokes equations numerically, using the boundaryintegral method. Their numerical results agree well with the lubrication approximation so long as the capillary number is small. Schwartz and Weidner [12] used curvilinear coordinates to model the flow of a thin film over an arbitrary one-dimensional curved substrate. Their governing equation is nevertheless analogous to that of Stillwagon and Larson; we will show that it is valid only if the substrate curvature is small. They also used a Green's function approach to analyse the small-time evolution of an initially uniform film. This approach was extended in [13] to flow over a two-dimensional substrate with small topography.

Flow on a circular cylinder has been studied, for example, by Bretherton [14] and by Hammond [15], while gravity (with the cylinder either vertical or horizontal) is incorporated in [16–19]. The analysis is fairly easily extended to flow on a perturbed circular cylinder. Gauglitz and Radke [20], for example, modelled the evolution of a thin film lining a slowly-varying cylindrical pore, while Jensen [21] considered a thin film inside a slightly bent cylindrical tube.

We consider the flow of a thin film over an arbitrary moving curved substrate. Our scaling assumptions are that the film thickness is much smaller than the radius of curvature of the substrate; that the capillary number, based on the substrate velocity, is small; and that the Reynolds number is small enough for inertia to be negligible throughout. These assumptions allow us to use a modified lubrication theory, expressed in a curvilinear coordinate system that is fixed in the moving substrate.

We identify three distinguished limits. First, if the substrate curvature is small, then we obtain a modified Landau-Levich equation, forced by the gradient in the substrate curvature, as in [8]. Second, if the substrate curvature is constant but not small, then the equation acquires a forcing term proportional to the gradient in the film thickness. This second regime applies to flow on a circular cylinder, and the extra term alluded to provides the destabilising mechanism that gives rise to the so-called Rayleigh instability, after [22]. It also applies if the substrate has nearly constant curvature, as in [20, 21].

The third distinguished limit occurs when the substrate has large, nonuniform curvature, whose gradient provides a forcing that dominates the leading-order flow. Thus, the film thickness satisfies a hyperbolic equation, whose solution is readily found using the method of characteristics. Capillarity enters only in quasi-steady inner regions where the hyperbolic solution becomes singular. This final case has not received much attention in the literature, and we concentrate on it for most of the paper.

This problem was also analysed, for the case of a stationary substrate, by Roy *et al.* [23]. Their approach is to include higher-order terms in the expansions to obtain a 'composite' model, assumed to be valid throughout the flow domain, that is solved numerically. Instead, we consider only the leading-order equations, identify the regions where they become invalid, and analyse the corresponding inner problems using matched asymptotic expansions. This allows us to identify the different asymptotic regimes outlined above, to obtain general analytical results concerning the possible formation of capillary shocks and/or puddles and to find the generic local behaviour near such singularities.

Since the substrate topography is manifested as a body force in the plane of the film, there is an analogy with other driven thin films. For example, Huppert [24] examined the gravity-driven flow of a thin layer of liquid down a tilted, flat substrate. The gravitational forcing results in wave steepening and, eventually, a theoretically discontinuous film thickness at the advancing contact line. The discontinuity is smoothed out locally by capillarity, as shown using matched asymptotic expansions by Troian *et al.* [25], who avoided the difficulty associated with the advancing contact line by supposing that it is proceeded by a very thin precursor layer. A similar approach was adopted by Moriarty *et al.* [26], who showed that analogous behaviour arises if the forcing is provided by rotation of the substrate or by blowing air on the surface.

In Section 2, the leading-order equation for flow over a moving curved surface is derived, using curvilinear coordinates that are fixed in the substrate. The derivation is simplified by assuming that the coordinate axes are lines of curvature of the substrate, as in [27]. However, the equations, once derived, are cast in an invariant form that is independent of the parametrisation chosen, so long as the coordinates are fixed in the substrate.

In Section 3, we focus on the case of a rigid substrate, and identify three distinct parameter regimes, depending on whether the substrate curvature is: (i) small, (ii) large, but nearly constant, or (iii) large, and not nearly constant. In Section 4 we restrict our attention to surfaces with only one spatial parameter, an example of which is a two-dimensional substrate as considered in [12]. We find a general analytical solution for the flow, and show that it predicts finite-time blow-up and for shock formation. Regularised inner equations that smooth out such singularities are found and matched with the outer flow. These effects are illustrated in Section 5 via reference to flow on a torus. Their generalisations for flow on an arbitrary rigid substrate are discussed in Section 6. In Section 7 we derive the equations for flow over a moving, axisymmetric surface, a configuration of interest in pulmonary airway reopening [28].

2. General equations of motion

2.1. Geometry of the substrate

Consider a moving substrate whose surface is given by

$$\boldsymbol{r} = \boldsymbol{r}_c(x_1, x_2; t),$$

where x_1 and x_2 are spatial parameters and t is time. We define the unit vectors

$$\boldsymbol{e}_1 = \frac{1}{a_1}\frac{\partial \boldsymbol{r}_c}{\partial x_1}, \quad \boldsymbol{e}_2 = \frac{1}{a_2}\frac{\partial \boldsymbol{r}_c}{\partial x_2}, \quad \boldsymbol{n} = \boldsymbol{e}_1 \wedge \boldsymbol{e}_2, \tag{1}$$

where

$$a_1 = \left|\frac{\partial \boldsymbol{r}_c}{\partial x_1}\right|, \quad a_2 = \left|\frac{\partial \boldsymbol{r}_c}{\partial x_2}\right|, \tag{2}$$

and $\boldsymbol{n}$ is the unit normal to the surface. To simplify the derivations we assume that x_1 and x_2 parametrise *lines of curvature* of the surface [29, p. 129], so that

$$\frac{\partial \boldsymbol{r}_c}{\partial x_1} \cdot \frac{\partial \boldsymbol{r}_c}{\partial x_2} = 0 \quad \text{and} \quad \frac{\partial^2 \boldsymbol{r}_c}{\partial x_1 \partial x_2} \cdot \boldsymbol{n} = 0.$$

We note that this parametrisation is singular at isolated umbilic points of the surface, where $a_1 a_2$ is equal to zero. The possibility that the coordinate system has an isolated singularity does not in fact impede the solution of the governing equation (22), so long as one is careful to discard any spurious singular solutions; an example is given in Section 4.3.

Now consider a thin liquid film flowing over the substrate. We use the coordinates (x_1, x_2, n) to describe a point in the liquid whose position is

$$\boldsymbol{r}(x_1,x_2,n;t)=\boldsymbol{r}_c(x_1,x_2;t)+n\boldsymbol{n}(x_1,x_2;t). \tag{3}$$

It is readily verified that this coordinate system is orthogonal, with scaling factors

$$\left|\frac{\partial \boldsymbol{r}}{\partial x_1}\right|=l_1=a_1(1-\kappa_1 n),\qquad \left|\frac{\partial \boldsymbol{r}}{\partial x_2}\right|=l_2=a_2(1-\kappa_2 n),\qquad \left|\frac{\partial \boldsymbol{r}}{\partial n}\right|=l_3=1, \tag{4a,b,c}$$

where κ_1 and κ_2 are the principal normal curvatures of the substrate [29, p. 129] in the directions parameterised by x_1 and x_2, respectively.

We resolve the velocity of the moving coordinate system onto the x_1-, x_2- and n-directions:

$$\frac{\partial \boldsymbol{r}_c}{\partial t}=v_1\boldsymbol{e}_1+v_2\boldsymbol{e}_2+v_3\boldsymbol{n}, \tag{5}$$

where the time derivative is taken with x_1 and x_2 fixed. These velocity components can be related to the rate of change of the first and second fundamental forms via certain geometric identities (see [27] for more details), including

$$a_2\frac{\partial a_1}{\partial t}=a_2\frac{\partial v_1}{\partial x_1}+v_2\frac{\partial a_1}{\partial x_2}-a_1a_2\kappa_1 v_3,\qquad a_1\frac{\partial a_2}{\partial t}=a_1\frac{\partial v_2}{\partial x_2}+v_1\frac{\partial a_2}{\partial x_1}-a_1a_2\kappa_2 v_3, \tag{6a,b}$$

$$\frac{\partial}{\partial t}(a_1\kappa_1)=\frac{\partial}{\partial x_1}\left(\frac{1}{a_1}\frac{\partial v_3}{\partial x_1}+\kappa_1 v_1\right)+\frac{1}{a_2}\frac{\partial a_1}{\partial x_2}\left(\frac{1}{a_2}\frac{\partial v_3}{\partial x_2}+\kappa_2 v_2\right), \tag{6c}$$

$$\frac{\partial}{\partial t}(a_2\kappa_2)=\frac{\partial}{\partial x_2}\left(\frac{1}{a_2}\frac{\partial v_3}{\partial x_2}+\kappa_2 v_2\right)+\frac{1}{a_1}\frac{\partial a_2}{\partial x_1}\left(\frac{1}{a_1}\frac{\partial v_3}{\partial x_1}+\kappa_1 v_1\right). \tag{6d}$$

2.2. FLUID MECHANICS

We denote the fluid pressure by p, the fluid velocity components by u_i, and the velocity of the fluid relative to the moving coordinate system by $\tilde{u}_i$, *i.e.*, $u_i = v_i + \tilde{u}_i$. We suppose that the thickness of the liquid layer is h, so that the free surface of the liquid is given by $n = h(x_1, x_2, t)$. We assume throughout that inertia can be neglected, so that our governing equations are the Stokes equations, with appropriate free-surface conditions. The defining physical parameters for the liquid are therefore its viscosity μ and surface tension σ.

The substrate is assumed to have a typical radius of curvature a, and to vary over a length-scale L (which may or may not be the same as a) in the x_1- and x_2-directions. The liquid film is assumed to be thin so that, if the scaling for h is $\bar{h}$, then $\bar{h}/L=\epsilon\ll 1$. Finally, U denotes a typical substrate speed. This motivates the following nondimensionalisation of the equations and boundary conditions:

$$\begin{aligned}
&v_i=Uv_i',\quad i=1,2,3,\\
&x_i=Lx_i',\quad i=1,2;\quad n=\epsilon L n',\\
&\tilde{u}_i=\frac{\epsilon^2\sigma L}{\mu a}\tilde{u}_i',\quad i=1,2;\quad \tilde{u}_3=\frac{\epsilon^3\sigma L}{\mu a}\tilde{u}_3',\\
&\kappa_i=\frac{1}{a}\kappa_i';\quad p=P_1+\frac{\sigma}{a}p';\quad t=\frac{\mu a}{\epsilon^2\sigma}t',
\end{aligned} \tag{7}$$

where P_1 is the ambient pressure.

Before nondimensionalising, we deduce an exact flux conservation equation from the continuity equation, $\nabla \cdot \boldsymbol{u} = 0$ or, in our coordinate system,

$$\frac{\partial}{\partial x_1}(l_2 u_1) + \frac{\partial}{\partial x_2}(l_1 u_2) + \frac{\partial}{\partial n}(l_1 l_2 u_3) = 0, \tag{8}$$

continuity of normal velo city with the substrate,

$$\tilde{u}_3 = 0 \quad \text{on} \quad n = 0 \tag{9}$$

and the kinematic condition on the free surface,

$$\tilde{u} = \frac{\partial h}{\partial t} + \frac{1}{l_1}\frac{\partial h}{\partial x_1}\left\{\tilde{u}_1 + h\left(\kappa_1 v_1 + \frac{1}{a_1}\frac{\partial v_3}{\partial x_1}\right)\right\} + \frac{1}{l_2}\frac{\partial h}{\partial x_2}\left\{\tilde{u}_2 + h\left(\kappa_2 v_2 + \frac{1}{a_2}\frac{\partial v_3}{\partial x_2}\right)\right\} \quad \text{on } n = h. \tag{10}$$

Integration of (8) with respect to n and application of the two boundary conditions (9) and (10) results in a single equation, respresenting net conservation of mass. This equation may be simplified using (6) and thus written in the form

$$\frac{\partial M}{\partial t} + \frac{\partial Q_1}{\partial x_1} + \frac{\partial Q_2}{\partial x_2} = 0, \tag{11}$$

where the 'film density' M and flux (Q_1, Q_2) are defined to be

$$M = \int_0^h l_1 l_2 \mathrm{d}n, \tag{12}$$

$$Q_1 = \int_0^h l_2 \left\{\tilde{u}_1 + n\left(\frac{1}{a_1}\frac{\partial v_3}{\partial x_1} + \kappa_1 v_1\right)\right\} \mathrm{d}n, \tag{13a}$$

$$Q_2 = \int_0^h l_1 \left\{\tilde{u}_2 + n\left(\frac{1}{a_2}\frac{\partial v_3}{\partial x_2} + \kappa_2 v_2\right)\right\} \mathrm{d}n. \tag{13b}$$

The Stokes equations, nondimensionalised according to (7), take the form (dropping primes)

$$\frac{\partial p}{\partial n} = O\left(\epsilon^2, \epsilon \mathrm{Ca}\frac{a}{L}\right), \tag{14}$$

$$\frac{1}{a_1}\frac{\partial p}{\partial x_1} = \frac{\partial^2 \tilde{u}_1}{\partial n^2} + O\left(\epsilon^2, \frac{\epsilon L}{a}, \mathrm{Ca}\frac{a}{L}\right), \tag{15a}$$

$$\frac{1}{a_2}\frac{\partial p}{\partial x_2} = \frac{\partial^2 \tilde{u}_2}{\partial n^2} + O\left(\epsilon^2, \frac{\epsilon L}{a}, \mathrm{Ca}\frac{a}{L}\right), \tag{15b}$$

where $\mathrm{Ca} = \mu U/\sigma$ is the capillary number. For the moment, ϵ and Ca are taken as independent small parameters but, in Section 7, we relate them for a regime of interest in pulmonary airway reopening.

For simplicity, in the analysis to follow we take the coordinate system to be fixed in the moving substrate, so that the no-slip condition reads

$$\tilde{u}_1 = \tilde{u}_2 = 0 \quad \text{on} \quad n = 0. \tag{16}$$

This assumption restricts the substrate motions to ones that preserve its principle directions; in the Appendix we show that this restriction is, in fact, unnecessary.

The balance between normal stress and surface tension on the free surface gives

$$p = -\mathcal{K} + O\left(\epsilon^2, \epsilon \mathrm{Ca}\frac{a}{L}\right) \quad \text{on} \quad n = h, \tag{17}$$

where $\mathcal{K}$ is twice the mean curvature (*i.e.*, the sum of the principal curvatures) of the free surface. The general expression for $\mathcal{K}$ is extremely complicated, but it may be expanded for small ϵ to give

$$\mathcal{K} \sim \kappa_1 + \kappa_2 + \frac{\epsilon a}{L}\nabla_s^2 h + \frac{\epsilon L}{a}\left(\kappa_1^2 + \kappa_2^2\right) h + O(\epsilon^2), \tag{18}$$

where ∇_s^2 is the surface Laplacian with respect to the substrate:

$$\nabla_s^2 h = \frac{1}{a_1 a_2}\left\{\frac{\partial}{\partial x_1}\left(\frac{a_2}{a_1}\frac{\partial h}{\partial x_1}\right) + \frac{\partial}{\partial x_2}\left(\frac{a_1}{a_2}\frac{\partial h}{\partial x_2}\right)\right\}.$$

The tangential stress balance may be written as

$$\frac{\partial \tilde{u}_1}{\partial n} + \frac{\mathrm{Ca}}{\epsilon}\frac{a}{L}\frac{1}{a_1}\frac{\partial v_3}{\partial x_1} + \frac{\mathrm{Ca}}{\epsilon}\kappa_1 v_1 = O\left(\epsilon^2, \frac{\epsilon L}{a}, \mathrm{Ca}\frac{a}{L}\right), \tag{19a}$$

$$\frac{\partial \tilde{u}_2}{\partial n} + \frac{\mathrm{Ca}}{\epsilon}\frac{a}{L}\frac{1}{a_2}\frac{\partial v_3}{\partial x_2} + \frac{\mathrm{Ca}}{\epsilon}\kappa_2 v_2 = O\left(\epsilon^2, \frac{\epsilon L}{a}, \mathrm{Ca}\frac{a}{L}\right), \tag{19b}$$

on $n = h$. More details of the equations and boundary conditions in this coordinate system can be found in [27]. From (14) and (17), we find

$$p = -\mathcal{K}(x_1, x_2, t) + O\left(\epsilon^2, \epsilon \mathrm{Ca}\frac{a}{L}\right). \tag{20}$$

Moreover, solving (15) for $\tilde{u}_1$ and $\tilde{u}_2$, using the boundary conditions (16) and (19), we obtain asymptotic expressions for the flux components (made dimensionless with $\epsilon^3 \sigma L^2/\mu a$):

$$Q_1 = -\frac{h^3}{3}\frac{a_2}{a_1}\frac{\partial p}{\partial x_1} + O\left(\epsilon^2, \frac{\epsilon L}{a}, \mathrm{Ca}\frac{a}{L}\right), \tag{21a}$$

$$Q_2 = -\frac{h^3}{3}\frac{a_1}{a_2}\frac{\partial p}{\partial x_2} + O\left(\epsilon^2, \frac{\epsilon L}{a}, \mathrm{Ca}\frac{a}{L}\right). \tag{21b}$$

The governing equation (11) for the film thickness h therefore reads, to leading order,

$$\frac{1}{a_1 a_2}\frac{\partial}{\partial t}(a_1 a_2 h) + \nabla_s \cdot \left(\frac{h^3}{3}\nabla_s \mathcal{K}\right) = O\left(\epsilon^2, \frac{\epsilon L}{a}, \mathrm{Ca}\frac{a}{L}\right), \tag{22}$$

where ∇_s is the surface gradient operator (again, with respect to the substrate):

$$\nabla_s \mathcal{K} = \frac{\partial \mathcal{K}}{\partial x_1}\frac{\boldsymbol{e}_1}{a_1} + \frac{\partial \mathcal{K}}{\partial x_2}\frac{\boldsymbol{e}_2}{a_2}, \qquad \nabla_s \cdot (q_1 \boldsymbol{e}_1 + q_2 \boldsymbol{e}_2) = \frac{1}{a_1 a_1}\left\{\frac{\partial}{\partial x_1}(a_2 q_1) + \frac{\partial}{\partial x_2}(a_1 q_2)\right\}.$$

Notice that, if the asymptotically small terms in Equation (1) of [23] are neglected, it reduces to (22).

3. Rigid substrate

3.1. Small curvature

Here we consider the case in which the substrate is both rigid and relatively flat, so that the curvature of the substrate is of the same order as the curvature of the thin film. The appropriate scaling choice is $L/a = \epsilon$ and, in this regime, plane Cartesian coordinates can be used to describe the surface, at least locally. The resulting equation is

$$\frac{\partial h}{\partial t} + \nabla \cdot \left(\frac{h^3}{3} \nabla (\kappa + \nabla^2 h) \right) = O(\epsilon^2), \tag{23}$$

where $\kappa = \kappa_1 + \kappa_2$ is twice the mean substrate curvature. If $\kappa = 0$, Equation (23) reduces to the classical lubrication equation for surface-tension-driven flow on a plane [7]. The two-dimensional restriction of (23) was derived in [8] and used in [12] to model paint flow over a surface with piecewise constant curvature. However, in cases where the curvature is not small, even if it is constant, Equation (23) is not asymptotically valid, as we will see in the next Section.

3.2. Constant (or nearly constant) curvature

If the substrate has constant mean curvature (for example if it is a circular cylinder), then the nondimensionalisation *ansatz* (7) has to be modified slightly. In this case we use the (constant) mean curvature curvature $1/a$ to define our lengthscale: $L = a$. The free-surface curvature, nondimensionalised with $1/a$, is then found to be

$$\mathcal{K} \sim 1 + \epsilon \left\{ \left(\kappa_1^2 + \kappa_2^2 \right) h + \nabla_s^2 h \right\} + O(\epsilon^2). \tag{24}$$

Now, since the flow is driven by the gradient of $\mathcal{K}$, the constant leading-order term in (24) is irrelevant. Effectively, the uniform capillary pressure associated with the substrate curvature may be absorbed into the ambient pressure P_1. The upshot is that an extra factor of ϵ must be included in the scaling for t, which becomes

$$t = \frac{\mu a}{\epsilon \sigma} t', \tag{25}$$

and the leading-order equation for h then reads

$$\frac{\partial h}{\partial t} + \nabla_s \cdot \left\{ \frac{h^3}{3} \nabla_s \left[\left(\kappa_1^2 + \kappa_2^2 \right) h + \nabla_s h \right] \right\} = 0. \tag{26}$$

The first term in square brackets is always destabilising: for flow on a circular cylinder it gives rise to the so-called Rayleigh instability. This important effect was omitted in [12].

The revised scaling (25) for t also applies if the substrate mean curvature is *nearly* constant. If the substrate principal curvatures, nondimensionalised with $1/a$, take the form

$$\kappa_1 \sim \kappa_1^{(0)} + \epsilon \kappa_1^{(1)} + O(\epsilon^2), \quad \kappa_2 \sim \kappa_2^{(0)} + \epsilon \kappa_2^{(1)} + O(\epsilon^2), \tag{27}$$

where $\kappa_1^{(0)} + \kappa_2^{(0)} = 1$, then (22) becomes

$$\frac{\partial h}{\partial t} + \nabla_s \cdot \left\{ \frac{h^3}{3} \nabla_s \left[\kappa_1^{(1)} + \kappa_2^{(1)} + \left((\kappa_1^{(0)})^2 + (\kappa_2^{(0)})^2 \right) h + \nabla_s^2 h \right] \right\} = 0. \tag{28}$$

This is just a modification of (26) to include the forcing due to the perturbation in the substrate curvature.

Consider, for example, a perturbed circular cylinder, with

$$\boldsymbol{r}_c = \begin{pmatrix} (1 + \epsilon r(z, \theta)) \ \cos\theta \\ (1 + \epsilon r(z, \theta)) \ \sin\theta \\ z \end{pmatrix}, \tag{29}$$

where z and θ are cylindrical polar coordinates. The substrate curvatures in the z- and θ-directions are given approximately by

$$\kappa_z \sim \pm\epsilon r \pm \epsilon \frac{\partial^2 r}{\partial z^2}, \quad \kappa_\theta \sim 1 \pm \epsilon \frac{\partial^2 r}{\partial \theta^2},$$

where $+(-)$ corresponds to flow outside(inside) the cylinder. Substitution of these in (28) gives the governing equation for the flow of a thin film on this substrate as

$$\frac{\partial h}{\partial t} + \nabla \cdot \left(\frac{h^3}{3} \nabla \left(\nabla^2 (h \pm r) + (h \pm r) \right) \right) = 0, \tag{30}$$

where the gradient operator is $\nabla = (\partial/\partial z, \partial/\partial\theta)^T$. An axisymmetric version of (30) was used in [20] to model thin film flow in a constricted pore. The case $r \equiv 0$ was considered by Hammond [15], who examined the nonlinear evolution of the Rayleigh instability. Another example of a perturbed cylinder, namely a slightly bent circular cylinder, was studied by Jensen [21]. His governing equation is also a special case of (28).

3.3. LARGE CURVATURE

Now we consider the scaling $L = a$, so that the free-surface curvature is, to leading order, equal to the substrate curvature. The governing equation (22) takes the form, valid up to $O(\epsilon)$,

$$\frac{\partial h}{\partial t} + \nabla_s \cdot \left(\frac{h^3}{3} \nabla_s \kappa \right) = 0, \tag{31}$$

where the substrate curvature, $\kappa = \kappa_1 + \kappa_2$, is a given function of x_1 and x_2. The hyperbolic equation (31) for h can be solved with relative ease once the substrate geometry is given. It clearly predicts migration of fluid up the curvature gradient, accompanied by wave-steepening and the possibility of shock formation. It is degenerate at points where κ is stationary: at such points h either tends to zero like $t^{-1/2}$ or blows up in finite time, depending on whether the surface-Laplacian of κ, is positive or negative. Both this blow-up and shock formation are smoothed out in practice by higher-order corrections to the free-surface curvature which involve spatial derivatives of h and so regularise (31). In Section 4, we illustrate all these for a substrate dependent on just one spatial parameter.

3.4. SUMMARY

We have identified three distinct scaling regimes:

$$\frac{L}{a} \ll \sqrt{\frac{\bar{h}}{a}} \ll 1 \Rightarrow \text{ substrate curvature is negligible,} \tag{32a}$$

$$\frac{L}{a} \sim \sqrt{\frac{\bar{h}}{a}} \ll 1 \Rightarrow \text{ substrate curvature} \sim \text{film curvature,} \tag{32b}$$

$$\sqrt{\frac{\bar{h}}{a}} \ll \frac{L}{a} \lesssim 1 \Rightarrow \text{ substrate curvature dominates.} \tag{32c}$$

(In each case we also require $\bar{h}/L = \epsilon \ll 1$.) Of these, the first two have been considered fairly widely. We concentrate on the third, which has not, for the remainder of the paper.

4. One-spatial-parameter thin-film flow

4.1. Solution of the hyperbolic equation

We now consider the special case in which the spatial dependence of the curved substrate and the thin film flowing over it can both be described by just one variable. Therefore we neglect all x_2-derivatives and put $x_1 \equiv x$. From (22) the resulting equation of motion for the film is

$$a_1 a_2 \frac{\partial h}{\partial t} + \frac{\partial}{\partial x}\left(\frac{qh^3}{3}\right) = 0, \quad \text{where} \quad q = \frac{a_2}{a_1}\frac{\partial \kappa}{\partial x} \tag{33}$$

and κ is the substrate mean curvature, so that a_1, a_2 and q are all given functions of x.

The general solution of (33) can readily be found using the method of characteristics. If the initial film profile is $h_0(x)$, then for subsequent time it is

$$h = h_0(s)\frac{q(s)^{1/3}}{q(x)^{1/3}}, \tag{34}$$

where the equations of the characteristic projections $x = x(s, t)$, are given by

$$\int_s^x \frac{a_1(\xi)a_2(\xi)\mathrm{d}\xi}{q(s)^{2/3}q(\xi)^{1/3}} = t h_0(s)^2. \tag{35}$$

The location and type of singularities that the solution develops depend on the form of the function q and the initial film profile h_0. However, we can make the general statement that for sufficiently smooth q and nonzero h_0, (33) does not admit solutions in which $h \to 0$ in finite time. To fix ideas, for the remainder of this section we suppose that the film is uniform initially: $h_0 \equiv 1$.

The solution for h breaks down on the envelope of the characteristic projections. This is obtained by differentiating (35) with respect to s and solving the resulting equation simultaneously with (35), and the resulting envelope may be written as

$$t = t_s(s) = -\frac{3a_1(s)a_2(s)}{2q'(s)}. \tag{36}$$

Suppose the solution breaks down first at $t = t_c$, $s = s_c$, *i.e.*, the minimum of t_s occurs at $s = s_c$:

$$t_s(s_c) = t_c, \quad t_s'(s_c) = 0, \quad t_s''(s_c) = \alpha^2, \text{ say.} \tag{37}$$

We examine two possible types of breakdown separately. First, if $q(s_c) \neq 0$, then the intersection of the characteristic projections signals the formation of a shock, as is usual in such nonlinear hyperbolic equations. We examine this case in Section 4.2. If it happens that $q(s_c) = 0$, so that the curvature is stationary, then Equation (33) is locally degenerate and a different kind of singularity occurs, corresponding to the formation of a local puddle of liquid. This behaviour is considered in Section 4.3.

4.2. Local solution near a shock

Suppose the outer solution has a shock at $x = X(t)$. We perform a local rescaling,

$$x = X(t) + \epsilon^{1/3}\xi, \tag{38}$$

which introduces a correction to the free-surface curvature and results in the following inner equation in the neighbourhood of the shock:

$$\frac{\partial}{\partial \xi}\left\{\frac{h^3}{3}\left(\frac{q(X)}{a_1(X)a_2(X)} + \frac{1}{a_1(X)^4}\frac{\partial^3 h}{\partial \xi^3}\right) - \dot{X}h\right\} = O(\epsilon^{1/3}). \tag{39}$$

Note that, over this new lengthscale, the film is in the regime identified in Section 3.1. Thus, (39) can be obtained either by scaling (22) appropriately or from (23).

By integrating (39) with respect to ξ, we have, to leading order,

$$\frac{h^3}{3}\left(\frac{q}{a_1a_2} + \frac{1}{a_1^4}\frac{\partial^3 h}{\partial \xi^3}\right) - \dot{X}h = f(t), \tag{40}$$

where f is arbitrary and, here and henceforth, the argument X is assumed. The boundary conditions for (40) are

$$h \to h_{\pm} \quad \text{as} \quad \xi \to \pm\infty, \tag{41}$$

where $h_{\pm}$ are the values of h that the outer solution sees at $x = X\pm$. Hence

$$\dot{X} = \frac{q}{3a_1a_2}\left(h^2 + h_+h_- + h_-^2\right), \tag{42}$$

which is the Rankine-Hugoniot relation for the conservation law (33), and

$$f = -\frac{q}{3a_1a_2}h_+h_-(h_+ + h_-). \tag{43}$$

Moreover (40) can be integrated once, giving

$$\frac{3f}{2}\left[\frac{1}{h^2}\right]_-^+ + 3\dot{X}\left[\frac{1}{h}\right]_-^+ + \frac{q}{a_1a_2}[h]_-^+ = \frac{1}{a_1^4}\int_{-\infty}^{\infty}(h'')^2\,\mathrm{d}\xi, \tag{44}$$

which simplifies to

$$\frac{q}{2a_1a_2}\frac{(h_+ - h_-)^3}{h_+h_-} = -\frac{1}{a_1^4}\int_{-\infty}^{\infty}(h'')^2\,\mathrm{d}\xi < 0, \tag{45}$$

so that $(h_+ - h_-)$ must take the opposite sign to q.

Recall that the characteristic speed is

$$u_c = \frac{\partial}{\partial t}(x(s,t)) = \frac{qh^2}{a_1 a_2}, \tag{46}$$

and hence

$$\dot{X} - u_c = \begin{cases} (h_- - h_+)(h_- + 2h_+)\dfrac{q}{3a_1a_2}, & x > X, \\ (h_+ - h_-)(2h_- + h_+)\dfrac{q}{3a_1a_2}, & x < X. \end{cases} \tag{47}$$

Since, as noted above, $(h_+ - h_-)q < 0$, we deduce that the characteristics of the hyperbolic problem travel into the shock on either side (as a causality argument would also have predicted). The leading-order outer solution following shock formation may, therefore, be found by solving the hyperbolic equation on either side and moving the shock according to the Rankine-Hugoniot relation (42). Also, we can deduce that (i) the shock moves in the same direction as the local flux and, hence, (ii) the film thickness behind the shock is greater than that ahead.

To track the position of the shock it is useful to know the values of s corresponding to either side of the shock. By differentiating the characteristic equation (35) with respect to t and substituting for $\dot{X}$ from (42), we obtain ordinary differential equations for these values:

$$[3a_1(s_+)a_2(s_+) + 2tq'(s_+)]\dot{s}_+ = \quad q(s_+)^{1/3}\left(q(s_-)^{1/3} - q(s_+)^{1/3}\right)\left(q(s_-)^{1/3} + 2q(s_+)^{1/3}\right), \tag{48a}$$

$$[3a_1(s_-)a_2(s_-) + 2tq'(s_-)]\dot{s}_- = \quad q(s_-)^{1/3}\left(q(s_+)^{1/3} - q(s_-)^{1/3}\right)\left(q(s_+)^{1/3} + 2q(s_-)^{1/3}\right). \tag{48b}$$

Initial conditions are found by expanding about $s = s_c$, $t = t_c$. The result is

$$s_\pm \sim s_c \pm \frac{\sqrt{6(t - t_c)}}{\alpha} \quad \text{as } t \searrow t_c. \tag{49}$$

We give an example, in which (48) and (49) are used to track the propagation of a shock, below in Section 5.

The leading-order inner solution for h can be written in the form

$$h = \frac{h_+ + h_-}{2} + \frac{h_+ - h_-}{2}\mathcal{H}(\zeta;\beta), \tag{50}$$

where

$$\zeta = \left(\frac{-2q}{a_2(h_+ - h_-)}\right)^{1/3} a_1\xi, \quad \beta = \frac{h_+ + h_-}{h_+ - h_-}, \tag{51}$$

and $\mathcal{H}$ satisfies the canonical problem

$$\mathcal{H}_{\zeta\zeta\zeta} = -\frac{(1+\mathcal{H})(1-\mathcal{H})(3\beta + \mathcal{H})}{(\beta + \mathcal{H})^3}, \quad \mathcal{H} \to \pm 1 \quad \text{as } \zeta \to \pm\infty. \tag{52}$$

We have assumed implicitly that (52) has a solution. Although we have not established this rigorously, by linearising about $\mathcal{H} = \pm 1$, it is straight forward to show that there is a one-parameter family of solutions satisfying each of $\mathcal{H} \to \pm 1$ as $\zeta \to \pm\infty$. Hence, one can

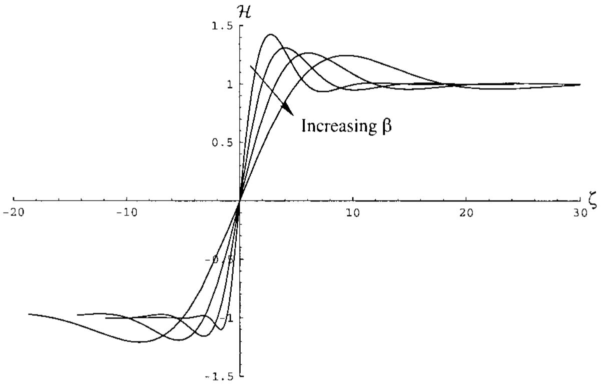

Figure 1. Solutions of the boundary-value problem (52) for $\beta = 2, 4, 8, 16$; the wave gets longer as β increases. The arbitrary translation is chosen such that they all pass through the origin.

shoot from (for example) $\zeta = -\infty$ and adjust the free parameter until the required behaviour at $\zeta = +\infty$ is obtained. Typical shock profiles resulting from this procedure are shown in Figure 1. They exhibit capillary waves both up- and downstream of the shock.

It is not immediately clear from (50) and (52) that h remains positive for all β. Note that h reaches zero at a finite value of ξ if $\mathcal{H}$ reaches $-\beta$, so that the denominator of (52) becomes infinite. Although we have not established this rigorously, it appears that (52) does not admit such solutions.

The boundary-value problem (52) is equivalent to the quasi-steady problem studied by Troian *et al.* [25] near an advancing contact line, although they were particularly concerned with the case where the 'precursor' film ahead of the propagating front is very thin, *i.e.*, with the limit $\beta \to 1$.

4.3. Local solution near a critical line

Now consider the flow in the neighbourhood of a value of x (without loss of generality $x = 0$) at which $q = 0$. Note that a fixed value of x in this two-dimensional analysis corresponds in general to a line on a three-dimensional substrate. The exception occurs if $a_2(0) = 0$, in which case $x = 0$ labels a point, not a line. This is illustrated by the ellipsoid of revolution

$$\boldsymbol{r}_c = \begin{pmatrix} a \sin\theta \cos\phi \\ a \sin\theta \sin\phi \\ b \cos\theta \end{pmatrix}.$$

If $a > b$, the ellipsoid is oblate. For flow on the outside of such an ellipsoid, κ is maximum at $\theta = 0$ and minimum at $\theta = \pi/2$. These are reversed if the flow is on the inside rather than the outside or if the ellipsoid is prolate: $a < b$. Now note that $a_\phi = a \sin\theta$ is zero at $\theta = 0$, which labels a point (this is an umbilic point of the surface), while $\theta = \pi/2$ labels a line.

For the remainder of this section we assume $a_2(0) \neq 0$, so that $x = 0$ labels a line; point maxima of κ are considered in Section 6.3. We begin by analysing the singular behaviour predicted by the hyperbolic equation (22) in the neighbourhood of $x = 0$, before performing an appropriate rescaling to recover the higher spatial derivatives that regularise the problem locally.

Suppose that q has the generic local behaviour

$$q \sim -a_1(0)a_2(0)\lambda x + O(x^3) \quad \text{as } x \to 0, \tag{53}$$

where $\lambda > 0$ so that $x = 0$ is a local maximum of the mean curvature and, for simplicity, the substrate is assumed to be symmetric about $x = 0$, so that the coefficient of x^2 is zero. The following analysis may readily be extended to account for more general local substrate geometry. By substituting $x = 0$ in (33), we find that the thickness at the origin satisfies the ordinary differential equation

$$\frac{\partial h}{\partial t}(0, t) = \frac{\lambda}{3} h(0, t)^3$$

and, therefore, blows up in finite time, namely

$$t_c = \frac{3}{2\lambda}.$$

This is, of course, the same time as given in (36) by looking for crossing of the characteristic projections. Moreover, the assumption of substrate symmetry implies that $x = 0$ is a local minimum of the characteristic envelope.

Near blow-up, the local behaviour of the outer solution for h is described by a similarity solution of

$$\frac{\partial h}{\partial t} = \frac{\lambda}{3}\frac{\partial}{\partial x}(x h^3), \tag{55}$$

which takes the form

$$x = \frac{C\sqrt{3 + 2\lambda(t - t_c)h^2}}{h^4}, \tag{56}$$

where C is an arbitrary constant. For $t < t_c$, h is smooth at $x = 0$, with

$$h \sim \sqrt{\frac{3}{2\lambda(t_c - t)}}\left\{1 - \frac{27x^2}{32C^2\lambda^4(t_c - t)^4} + \cdots\right\} \quad \text{as } x \to 0. \tag{57}$$

For fixed $x > 0$, h approaches the following singular behaviour at blow-up:

$$h \sim \frac{3^{1/8}C^{1/4}}{x^{1/4}}\left\{1 + \frac{\sqrt{C}\lambda(t - t_c)}{4 \times 3^{3/4}\sqrt{x}} + \cdots\right\} \quad \text{as } t \to t_c. \tag{58}$$

Finally, for $t > t_c$, the behaviour of h near the origin is

$$h \sim \frac{C^{1/3}(2\lambda(t - t_c))^{1/6}}{x^{1/3}}\left\{1 + \frac{x^{2/3}}{2C^{2/3}(2\lambda(t - t_c))^{4/3}} + \cdots\right\} \tag{59}$$

as $x \to 0$.

Blow-up first occurs at $t = t_c$, when the characteristic projections with $s > 0$ start to cross $x = 0$. We label the characteristic projection that crosses $x = 0$ at time t by $s = s_0(t)$. According to (35), S_0 satisfies

$$\int_0^{s_0} \frac{a_1(\xi)a_2(\xi)\,\mathrm{d}\xi}{q(\xi)^{1/3}} = -2q(s_0)^{2/3},$$

which may be differentiated with respect to t to obtain the following ordinary differential equation for $s_0(t)$:

$$(t_s(s_0) - t)\dot{s}_0 = \frac{3q(s_0)}{2q'(s_0)}. \tag{60}$$

Recall that $t_s(s)$ is the characteristic envelope defined by (36); here $s_c = 0$ and $t_s''(0) = \alpha^2$. The initial condition for (60) is found by expanding $t_s(s_0)$ about $s_0 = 0$, which gives

$$s_0 \sim \frac{2}{\alpha}\sqrt{2(t - t_c)} \quad \text{as } t \searrow t_c. \tag{61}$$

The inner behaviour of the outer solution for h is

$$h = \frac{q(s_0)^{1/3}}{q(x)^{1/3}} \sim -\frac{q(s_0)^{1/3}}{[a_1(0)a_2(0)\lambda]^{1/3}x^{1/3}}\left(1 + O(x^2)\right) \tag{62}$$

as $x \to 0$, $t > t_c$. Substitution of (61) in (62) gives the following local behaviour as $x \to 0$, $t \searrow t_c$,

$$h \sim -\frac{\sqrt{2}(t - t_c)^{1/6}}{\alpha^{1/3}x^{1/3}}\left(1 + O(x^2)\right),$$

and comparison with (59) allows us to identify the constant C:

$$C = \frac{2}{\alpha\sqrt{\lambda}}. \tag{63}$$

Now, the blow-up predicted by the hyperbolic equation (33) must be smoothed out in some inner region where (33) is regularised by higher spatial derivatives of h. As in Section 4.2, the correct lengthscale is chosen by ensuring that the substrate and free-surface curvature terms balance in (22), resulting in

$$h = \epsilon^{-1/5}H, \quad x = \epsilon^{1/5}\xi, \quad q = \epsilon^{1/5}\tilde{q}, \tag{64}$$

where

$$\tilde{q} \sim -\lambda\xi + O(\epsilon^{2/5}). \tag{65}$$

The inner equation for H is therefore

$$a_1(0)a_2(0)\epsilon^{2/5}\frac{\partial H}{\partial t} + \frac{\partial}{\partial \xi}\left(\frac{H^3}{3}\left([a_2(0)a_1(0)^{-3}O(\epsilon^{1/5})]H_{\xi\xi\xi} - \lambda\xi\right)\right) = O(\epsilon^{3/5}). \tag{66}$$

Matching with the outer solution requires

$$H \sim -\frac{q(s_0)^{1/3}}{\lambda^{1/3}\xi^{1/3}}\epsilon^{2/15} \quad \text{as } \xi \to \infty \tag{67}$$

while, assuming symmetry about the origin, we have $H_\xi(0) = H_{\xi\xi\xi}(0) = 0$. Hence, setting $H = H_\xi = 0$ at $\xi = l$ to leading order,

$$H = \frac{\lambda a_1(0)^3}{24a_2(0)}(\xi^2 - l^2) \quad \xi < l. \tag{68}$$

The capillary static solution (68), which corresponds to a ‘puddle’ of liquid accumulated at the origin, cannot be matched directly with (67). Instead there must be a transition region between the two in the neighbourhood of $\xi = l$. As in many such problems where a thin layer of fluid flows into a static meniscus (*cf.* [30]) the matching of the free surface is nontrivial, requiring a formally infinite number of intermediate regions. Without doing so in detail, we can obtain an evolution equation for l by matching with the flux from the outer solution, whence

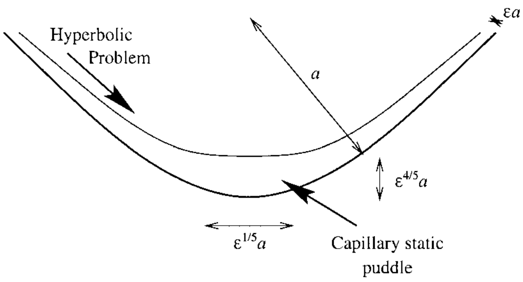

Figure 2. Schematic picture of a capillary static puddle.

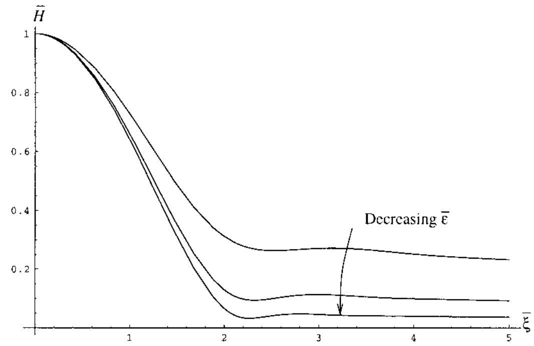

Figure 3. Local film profile $\bar{H}$ *vs.* $\bar{\xi}$, found by solving (71), for $\bar{\epsilon} = 10^{-3}, 10^{-6}, 10^{-9}$.

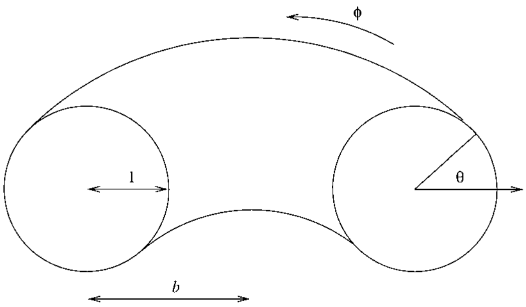

Figure 4. Definition sketch for a torus.

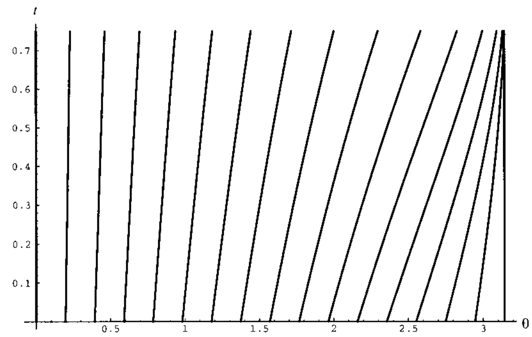

Figure 5. Characteristic projections for flow outside a torus with radius ratio $b = 2$.

$$\frac{\mathrm{d}}{\mathrm{d}t}\left(\frac{\lambda l^5 a_1(0)^4}{45}\right) = -\frac{q(s_0)}{3} \tag{69}$$

where the bracketed term is the volume of liquid per unit length in the x_2-direction (nondimensionalised with ϵa^2) that has accumulated at the critical line. The implication is that the fluid all ends up in a region of length $\epsilon^{1/5}a$ and thickness $\epsilon^{4/5}a$, as illustrated in Figure 2.

The local film profile may be visualised by solving the uniformly-valid quasi-static problem

$$H^3\left(\frac{a_2}{a_1^3}H_{\xi\xi\xi} - \lambda\xi\right) = -\epsilon^{2/5}q, \tag{70a}$$

$$H(0) = \frac{\lambda a_1^3 l^4}{24a_2}, \quad H_\xi(0) = 0, \quad H \sim -\frac{\epsilon^{2/15}q^{1/3}}{\lambda^{1/3}\xi^{1/3}} \text{ as } \xi \to \infty, \tag{70b}$$

where the arguments 0 for a_i and s_0 for q have been dropped for ease of notation. This may be reduced to the canonical problem

$$\bar{H}^3\left(\bar{H}_{\bar{\xi}\bar{\xi}\bar{\xi}} - \bar{\xi}\right) = \bar{\epsilon}^{2/5}, \tag{71a}$$

$$\bar{H}(0) = 1, \quad \bar{H}_{\bar{\xi}}(0) = 0, \quad \bar{H} \sim \frac{\bar{\epsilon}^{2/15}}{\bar{\xi}^{1/3}} \text{ as } \bar{\xi} \to \infty, \tag{71b}$$

where

$$H = \frac{\lambda a_1^3 l^4}{24 a_2}\bar{H}, \quad \xi = \frac{l}{24^{1/4}}\bar{\xi}, \quad \bar{\epsilon} = 24^{65/8}\epsilon\left(-\frac{a_1^9\lambda^4 l^{13}}{a_2^3 q}\right)^{5/2}. \tag{72}$$

We illustrate some solutions of (71), for various values of $\bar{\epsilon}$, in Figure 3. We see that the static meniscus in each case has a minimum value close to $\bar{\xi} = 24^{1/4} \approx 2{\cdot}213$, which tends to zero as $\bar{\epsilon} \to 0$. Only one capillary ridge is discernible between the puddle and the outer flow. These ridges correspond to the intermediate asymptotic regions alluded to previously; in general, the number of such regions increases as $\bar{\epsilon}$ decreases, varying like $\log(-\log\bar{\epsilon})/\log 10$.[1] Thus $\bar{\epsilon}$ has to be unphysically small before more than one is observed.

5. Example – flow on a torus

We illustrate the theory of Section 4 by analysing the flow of a thin film on the torus

$$\boldsymbol{r}_c = \begin{pmatrix} (b+\cos\theta)\ \cos\phi \\ (b+\cos\theta)\ \sin\phi \\ \sin\theta \end{pmatrix}, \tag{73}$$

where $b > 1$ is the ratio of the radii and $\theta \equiv x$, as illustrated in Figure 4. Flow on a torus was also considered by Roy *et al.* [23]. The metric coefficients are

$$a_\theta = 1, \quad a_\phi = b + \cos\theta, \tag{74}$$

and the substrate curvature is

$$\kappa = \pm\frac{b + 2\ \cos\theta}{b+\cos\theta}, \tag{75}$$

where $+(-)$ corresponds to flow inside(outside) the torus. Hence

$$q = \mp\frac{b\ \sin\theta}{b+\cos\theta}, \tag{76}$$

and the time to shock formation is

$$t_s = \pm\frac{3(b+\cos\ s)^3}{2b(1+b\ \cos\ s)} \tag{77}$$

where, as before, s is the characteristic coordinate.

For flow on the outside of a torus, *i.e.*, a negative sign in (77), the minimum value of t_s always occurs at $s = \pi$, where κ is maximum. Hence blow-up occurs at $\theta = \pi$ at time $t_c = 3(b-1)^2/2b$. The characteristic projections and film profile for such a flow with $b = 2$ (so that $t_c = 3/4$) are shown in Figures 5 and 6.

For flow inside a torus, *i.e.*, a positive sign in (77), the character of the solution depends on the size of b. For $b > 3$, the minimum of t_s occurs at $s = 0$, so that blow-up occurs at $\theta = 0$, $t_c = 3(1+b)^2/2b$. For $b < 3$, however, the first singularity to develop is a shock on the characteristic $s = s_c = \cos^{-1}((b^2-3)/2b)$ at time $t_s = 81(b^2-1)^2/8b^4$. The time t_s to formation of a singularity and corresponding characteristic coordinate s_c are plotted against b in Figure 7.

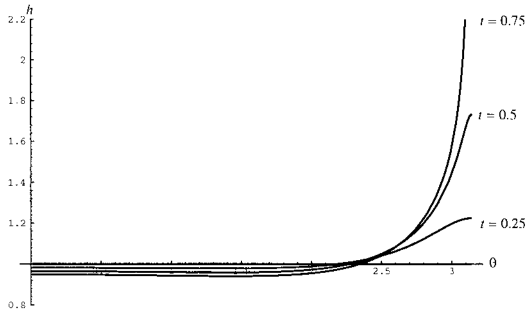

Figure 6. Solution for h on outside of torus with radius ratio $b = 2$.

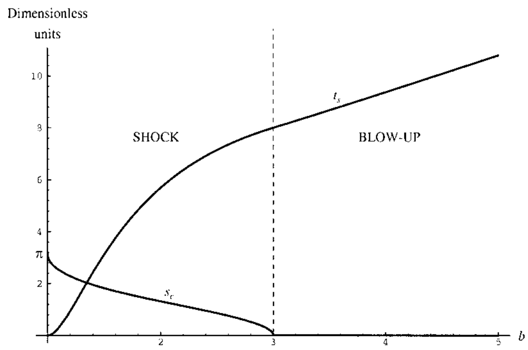

Figure 7. Time t_s to singularity formation, and corresponding characteristic coordinate s_c *vs.* radius ratio b for flow inside a torus.

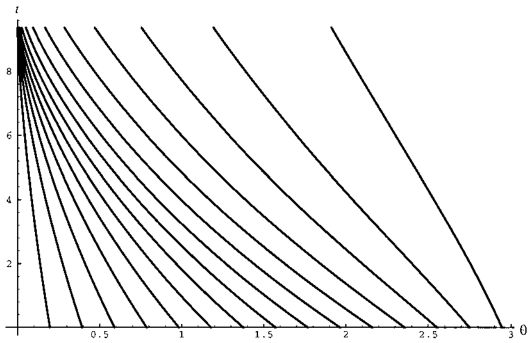

Figure 8. Characteristic projections for flow inside a torus with radius ratio $b = 4$.

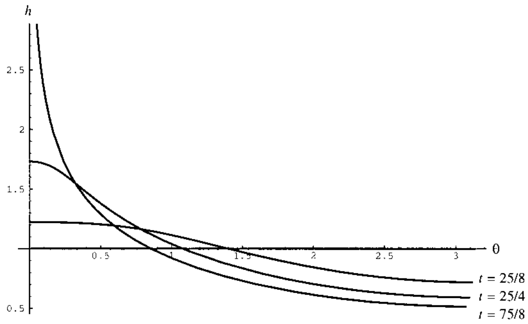

Figure 9. Solution for h on the inside of a torus with radius ratio $b = 4$.

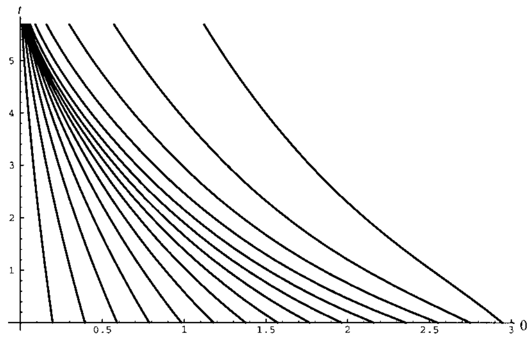

Figure 10. Characteristic projections for flow inside a torus with radius ratio $b = 2$.

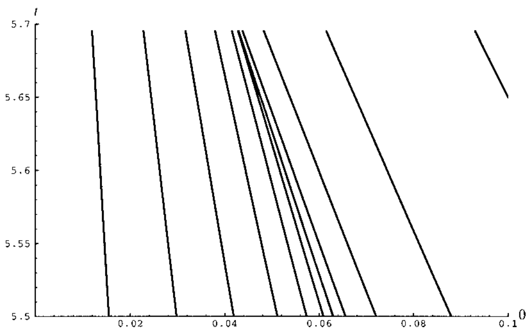

Figure 11. Detail from Figure 10, showing characteristics crossing.

The former of these two cases is illustrated in Figures 8 and 9, where characteristic projections and the film profile are shown for $b = 4$ (so $t_c = 75/8$). The characteristic projections for the case $b = 2$ (so $t_s = 729/128$, $s_c = \cos^{-1}(1/4)$, corresponding to $\theta \approx 0{\cdot}043$) are shown in Figure 10. In the detail shown in Figure 11, it is clearly seen that characteristics begin to cross before they reach the critical point $\theta = 0$.

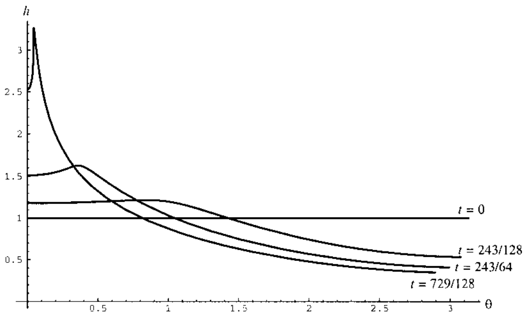

Figure 12. Solution for h on the inside of a torus with radius ratio $b = 2$.

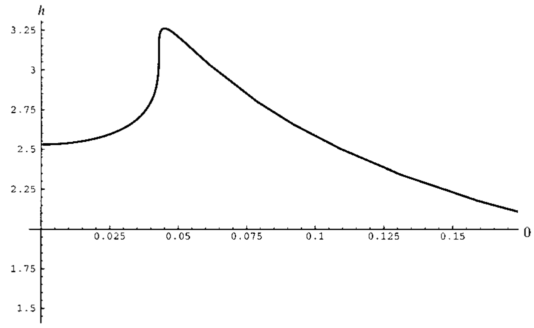

Figure 13. Detail from Figure 12 at $t = t_c = 729/128 \approx 5{\cdot}7$, showing shock.

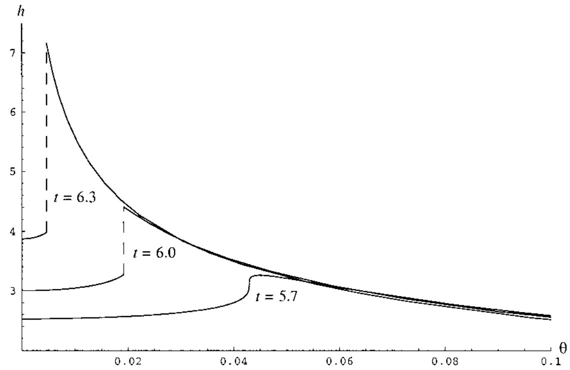

Figure 14. Solution for h on the inside of a torus with ratio $b = 2$, showing shock propagation.

That this signifies the formation of a shock is seen in the film profile shown in Figure 12, and the detail thereof in Figure 13.

To continue the solution further, we have to use (48) and (49) to move the shock, while solving the hyperbolic problem on either side. Thus, as shown in Figure 14, we can track the shock as it propagates round the torus.

6. Generalisation to arbitrary substrate geometry

6.1. Hyperbolic problem

Here we briefly describe the generalisation of the theory of Section 4 to flow over an arbitrary curved substrate. The general governing equation (22) may be written in the form

$$a_1 a_2 \frac{\partial h}{\partial t} + \frac{\partial}{\partial x_1}\left(\frac{q_1 h^3}{3}\right) + \frac{\partial}{\partial x_2}\left(\frac{q_2 h^3}{3}\right) = 0, \tag{78a}$$

where

$$q_1 = \frac{a_2}{a_1}\frac{\partial \kappa}{\partial x_1}, \quad q_2 = \frac{a_1}{a_2}\frac{\partial \kappa}{\partial x_2}. \tag{78b}$$

Since $q_1(x_1, x_2)$ and $q_2(x_1, x_2)$ are both *a priori* known functions, the problem for the streamlines $x_i = Z_i(\tau)$, namely

$$\dot{Z}_1 = \frac{q_1(Z_1, Z_2)}{a_1(Z_1, Z_2)a_2(Z_1, Z_2)}, \quad \dot{Z}_2 = \frac{q_2(Z_1, Z_2)}{a_1(Z_1, Z_2)a_2(Z_1, Z_2)}, \tag{79}$$

is a phase-plane problem which need only be solved once. The critical points of (79) are stagnation points of the flow, at which puddles of fluid will form if κ is a local maximum, as in Section 4.3.

The solution for h can be expressed in terms of the solution of the related steady hyperbolic problem for $\Phi(x_1, x_2)$ (which also need only be solved once)

$$\frac{\partial}{\partial x_1}(q_1\Phi) + \frac{\partial}{\partial x_2}(q_2\Phi) = 0. \tag{80}$$

It is then simple to show from (78) that $h/\Phi^{1/3}$ is constant along streamlines. Therefore

$$\frac{h(Z_1(\tau), Z_2(\tau))}{\Phi(Z_1(\tau), Z_2(\tau))^{1/3}} = \frac{h_0(Z_1(\tau_0), Z_2(\tau_0))}{\Phi(Z_1(\tau_0), Z_2(\tau_0))^{1/3}}, \tag{81}$$

where $h = h_0(x_1, x_2)$ at $t = 0$ and the material point that is currently at position τ along a streamline started at position τ_0. Hence τ and τ_0 are related in the following time-dependent way:

$$\int_{\tau_0}^{\tau} \frac{\mathrm{d}\tilde{\tau}}{\Phi(Z_1(\tilde{\tau}), Z_2(\tilde{\tau}))^{2/3}} = \frac{h_0(Z_1(\tau_0), Z_2(\tau_0))^2}{\Phi(Z_1(\tau_0), Z_2(\tau_0))^{2/3}} t. \tag{82}$$

In (81) and (82), the streamline along which τ varies is just a parameter. On each particular streamline, the time to shock formation is found by differentiating (82) with respect to τ_0:

$$t_s(\tau_0) = \left[-\frac{3a_1a_2h_0}{2((q_1h_0^3)_{x_1} + (q_2h_0^3)_{x_2})} \right]_{(Z_1(\tau_0), Z_2(\tau_0))}. \tag{83}$$

The material point that first forms a shock is found by minimising (83) as a function of Z_1 and Z_2.

6.2. Shock propagation

Now we generalise the theory of Section 4.2 to describe the propagation of a shock over an arbitrary surface. Suppose that the shock is parametrised by $x_i = X_i(s, t)$, where s is arc-length along the shock. We use the local coordinates

$$x_1 = X_1 + \epsilon^{1/3}\hat{n} \sin\theta, \quad x_2 = X_2 - \epsilon^{1/3}\hat{n} \cos\theta, \tag{84}$$

where

$$\frac{\partial X_1}{\partial s} = \cos\theta, \quad \frac{\partial X_2}{\partial s} = \sin\theta.$$

Define the velocity components of the shock

$$V_s = \frac{\partial X_1}{\partial t}\cos\theta + \frac{\partial X_2}{\partial t}\sin\theta, \qquad V_n = \frac{\partial X_1}{\partial t}\sin\theta - \frac{\partial X_2}{\partial t}\cos\theta, \tag{85a,b}$$

which are therefore related by

$$\frac{\partial V_s}{\partial s} + \frac{\partial \theta}{\partial s}V_n = 0, \quad \frac{\partial V_n}{\partial s} - \frac{\partial \theta}{\partial s}V_s = -\frac{\partial \theta}{\partial t}. \tag{86}$$

Transforming the governing equation (22) into the new coordinate system, the leading-order equation is found to be

$$\frac{h^3}{3}\left(A(s,t)\frac{\partial^3 h}{\partial \hat{n}^3} + B(s,t)\right) - V_n h = f(s,t), \tag{87}$$

where

$$A = \left(\frac{\cos^2\theta}{a_2^2} + \frac{\sin^2\theta}{a_1^2}\right)^2, \qquad B = \frac{\sin\theta}{a_1^2}\frac{\partial\kappa}{\partial x_1} - \frac{\cos\theta}{a_2^2}\frac{\partial\kappa}{\partial x_2}. \tag{88}$$

Matching with the outer solution on either side of the shock,

$$h \to h_\pm \quad \text{as } \hat{n} \to \pm\infty,$$

gives

$$f = -\frac{B}{3}h_+h_-(h_+ + h_-),$$

and the normal velocity

$$V_n = \frac{B}{3}(h_+^2 + H_+h_- + h_-^2). \tag{89}$$

The analysis of Section 4.2 can now be followed closely. By integrating (87) once, we deduce that $(h_+ - h_-)$ must take the opposite sign to B. The characteristic velocity is given by

$$\boldsymbol{u}_c = \begin{pmatrix} \dot{Z}_1 \\ \dot{Z}_2 \end{pmatrix} = \frac{h^2}{a_1^2 a_2^2}\begin{pmatrix} a_2^2\kappa_{x_1} \\ a_1^2\kappa_{x_2} \end{pmatrix},$$

and hence the component of the characteristic velocity across the shock on either side is

$$[\boldsymbol{u}_c \cdot \hat{\boldsymbol{n}}]_\pm = h_\pm^2 B. \tag{90}$$

This leads to the result, analogous to (47), that the characteristics flow into the shock on either side:

$$[\boldsymbol{u}_c \cdot \hat{\boldsymbol{n}}]_+ < V_n < [\boldsymbol{u}_c \cdot \hat{\boldsymbol{n}}]_-. \tag{91}$$

The regularised solution for h in the neighbourhood of the shock can be written in terms of the solution $\mathcal{H}$ of the canonical problem (52):

$$h = \frac{h_+ + h_-}{2} + \frac{h_+ - h_-}{2}\mathcal{H}(\nu;\beta), \quad \text{where} \quad \beta = \frac{h_+ + h_-}{h_+ - h_-}, \tag{92}$$

and

$$\nu = \left(\frac{-2B}{A(h_+ - h_-)}\right)^{1/3}\hat{n}. \tag{93}$$

In practice, once the hyperbolic problem has been solved on either side of the shock, the evolution of its position is determined by (86), where V_n is given by (89), and B by (88).

6.3. Local solution near a critical point

Consider a critical point (without loss of generality taken to be the origin) at which κ is stationary. Hence we can write κ in the form

$$\kappa \sim \text{ constant. } - \sum_{i,j=1}^{2} K_{ij} a_i(0) a_j(0) x_i x_j + \cdots . \tag{94}$$

An inner solution is sought via the scalings

$$h = \epsilon^{-1/3} H, \quad a_i(0) x_i = \epsilon^{1/6} \sum_{j=1}^{2} P_{ij} \xi_j, \tag{95}$$

where P_{ij} is a rotation tensor that diagonalises K_{ij}:

$$\boldsymbol{P}^T \boldsymbol{K} \boldsymbol{P} = \begin{pmatrix} \Lambda_1 & 0 \\ 0 & \Lambda_2 \end{pmatrix}. \tag{96}$$

The leading-order inner problem for H reads

$$\frac{\partial^2 H}{\partial \xi_1^2} + \frac{\partial^2 H}{\partial \xi_2^2} = \Lambda_1 \xi_1^2 + \Lambda_2 \xi_2^2 - C, \quad (\xi_1, \xi_2) \in \mathcal{D}, \tag{97}$$

where $\mathcal{D}$ is the region occupied by the puddle and C is an arbitrary constant (the scaled pressure drop across the quasi-static meniscus). As in Section 4.3, detailed matching with the outer solution is problematic but, to leading order, it is sufficient to impose that both H and its normal derivative be zero on the boundary of the puddle, that is

$$H = \frac{\partial H}{\partial \xi_1} = \frac{\partial H}{\partial \xi_2} = 0 \quad \text{on } \partial \mathcal{D}. \tag{98}$$

The problem (97, 98) is similar to the classical contact problem between a membrane and a plane under an applied pressure. By inspection we seek a solution of the form

$$H = (a\xi_1^2 + b\xi_2^2 - c)^2. \tag{99}$$

On substituting this in (97), a, b and c are found to satisfy

$$12a^2 + 4ab = \Lambda_1, \quad 12b^2 + 4ab = \Lambda_2, \quad 4(a+b)c = C. \tag{100}$$

The condition for a and b to be real is

$$\Lambda_1 (17 - 12\sqrt{2}) \Lambda_2 > 0 \quad \text{and} \quad \Lambda_2 + (17 - 12\sqrt{2}) \Lambda_1 > 0, \tag{101}$$

that is, there are only small sectors of (Λ_1, Λ_2) parameter-space in which a and b are real while Λ_1 and Λ_2 take different signs.

For $\mathcal{D}$ to be a bounded region we require a and b to take the same sign (without loss of generality +), and this can occur if and only if Λ_1 and Λ_2 are both positive, *i.e.*, if the origin is a true maximum of κ. The appropriate solutions of (100) are

$$a = \frac{\sqrt{\Lambda_2 + 17\Lambda_1 - \sqrt{\Lambda_1^2 + 34\Lambda_1\Lambda_2 + \Lambda_2^2}}}{8\sqrt{3}}, \tag{102a}$$

$$b = \frac{\sqrt{\Lambda_1 + 17\Lambda_2 - \sqrt{\Lambda_1^2 + 34\Lambda_1\Lambda_2 + \Lambda_2^2}}}{8\sqrt{3}}. \tag{102b}$$

In terms of these, the volume of liquid in the puddle (nondimensionalised with ϵL^3) is

$$V = \int\int_{\mathcal{D}} H \,\mathrm{d}\xi_1 \mathrm{d}\xi_2 = \frac{\pi}{192}\frac{C^3}{\sqrt{ab}(a+b)^3}. \tag{103}$$

As in (69), we can equate the rate of change of V to the flux of liquid into the origin predicted by the outer problem:

$$\frac{\mathrm{d}V}{\mathrm{d}t} = \oint_{\partial\mathcal{D}} \frac{h^3}{3}(q_2 \,\mathrm{d}x_1 - q_1 \,\mathrm{d}x_2), \tag{104}$$

where $\partial\mathcal{D}$ is a circuit of the origin which, in the outer region, is shrunk down to zero length.

7. Travelling-wave theory in an axisymmetric geometry

Now we apply the general theory derived in Section 2 to the case in which the substrate is axisymmetric. Put

$$\boldsymbol{r}_c = \begin{pmatrix} R(z,t)\ \cos\theta \\ R(z,t)\ \sin\theta \\ z \end{pmatrix}. \tag{105}$$

Then it is readily found that

$$a_z = \sqrt{1+R_z^2}, \quad a_\theta = R, \quad \kappa_z = -\frac{R_{zz}}{(1+R_z^2)^{3/2}}, \quad \kappa_\theta = \frac{1}{R\sqrt{1+R_z^2}}. \tag{106}$$

For the substrate velocity, we follow [5] and make the simplifying assumption of purely radial motion, so that

$$\boldsymbol{v} = \begin{pmatrix} R_t\ \cos\theta \\ R_t\ \sin\theta \\ 0 \end{pmatrix}. \tag{107}$$

This means that the coordinate system (z,θ) is fixed in the substrate, as required by the theory.

We seek solutions in which the film is axisymmetric as well as the substrate, so that (22) reduces to

$$\frac{\partial}{\partial t}\left(R\sqrt{1+R_z^2}h\right) + \frac{\partial}{\partial z}\left(\frac{h^3}{3}\frac{R}{\sqrt{1+R_z^2}}\frac{\partial\mathcal{K}}{\partial z}\right) = 0. \tag{108}$$

This is the general equation for thin-film flow on a moving axisymmetric substrate. It may admit further simplification if there is a disparity between the timescale for motion of the substrate and the timescale for surface tension levelling. We illustrate this by considering a travelling-wave solution of (108), *i.e.*, a solution that is steady in a frame moving with speed U in the z-direction, so that, in dimensionless terms,

$$\frac{\partial}{\partial t} = -\frac{\mathrm{Ca}}{\epsilon^2}\frac{a}{L}\frac{\partial}{\partial z}. \tag{109}$$

Then (108) can be integrated once to give

$$\frac{R}{\sqrt{1+R_z^2}}\frac{h^3}{3}\mathcal{K}_z - \frac{\mathrm{Ca}}{\epsilon^2}\frac{a}{L}Rh\sqrt{1+R_z^2} = \text{ constant.} \tag{110}$$

This governing equation is used in [28] to model the liquid lining of pulmonary airways.

From (110) we can identify three more scaling regimes to go with (32):

$$\epsilon^2\frac{L}{a} \ll \text{ Ca } \ll 1 \Rightarrow \text{ surface tension levelling is negligible,}$$

$$\epsilon^2\frac{L}{a} \sim \text{ Ca } \ll 1 \Rightarrow \text{ surface tension levelling} \sim \text{substrate motion,}$$

$$\text{Ca} \ll \epsilon^2\frac{L}{a} \ll 1 \Rightarrow \text{ substrate motion is negligible.}$$

These three regimes apply quite generally to flow on moving surfaces. The second case is particularly of interest for the film left behind a liquid bridge propagating along an elastic tube – the configuration considered in [28] – in which, as in [14], $L/a = O(\mathrm{Ca}^{1/3})$ and $\epsilon = O(\mathrm{Ca}^{1/3})$.

8. Conclusions

We have used systematic asymptotic expansions to derive the general leading-order equations governing the flow of a thin liquid film over a moving, curved substrate. We have identified the parameter regimes in which the various effects of substrate curvature, substrate motion and film curvature are or are not important. For relatively small substrate curvature, the film profile satisfies a fourth-order, nonlinear parabolic equation. For larger substrate curvature, the governing equation is hyperbolic, with the curvature of the film itself only becoming important in the neighbourhood of certain points or lines where the solution of the hyperbolic problem is singular. This decomposition of the film into an outer region, where the solution can be found using characteristics, and inner regions corresponding to shocks or localised 'puddles' enables us to make the following general statements about flow on any curved substrate.

1. The local behaviour near any shock is given by the quasi-steady problem (52). The shock moves according to the Rankine-Hugoniot condition (42) for one-dimensional flow or (89) in two dimensions.

2. After a finite time, capillary-static puddles form at local maxima of the substrate curvature. If this maximum occurs on a line, the puddle has width of order $\epsilon^{1/5}a$ and thickness or order $\epsilon^{4/5}$a. At a point maximum, a puddle forms with typical radius $\epsilon^{1/6}a$ and thickness $\epsilon^{2/3}a$. The leading-order puddle shapes are given by (68) and (99), respectively.

It is worth making a constrast between our approach and that adopted by Roy *et al.* [23]. They derive a governing equation that includes some higher-order corrections neglected in our leading-order equation (31). The extra terms include spatial derivatives that smooth out any singularities developed by the underlying hyperbolic problem (31). Thus their model equation may be solved numerically throughout the fluid domain. This pragmatic approach allows interesting nontrivial problems to be solved relatively easily, but does not distinguish the generic structures described above. Furthermore, it is asymptotically inconsistent. When the correction terms serve to smooth out singularities in the leading-order solution, they are having a leading-order effect. If this occurs, the asymptotic expansions used to derive the equation in the first place have become disordered, and there is no guarantee that the correct local behaviour is obtained simply by including further terms in the expansion.[2] Instead, inner expansions, in which different dominant balances prevail, should be constructed at such points of nonuniformity. This is the approach we follow in Sections 4.2 and 4.3.

Our general theory was illustrated first by considering one-dimensional flow on a torus. We found that, depending on the shape of the torus and whether the flow was on the inside or the outside, both shocks and puddles could be observed. Our second illustrative example concerned flow inside a moving axisymmetric substrate. This enabled us to identify the three parameter regimes for the substrate velocity under which (i) the film thickness responds only to substrate motion and surface tension is negligible; (ii) surface-tension-driven motion and substrate-driven motion of the film balance; (iii) surface-tension-driven flow dominates.

Much analysis remains to be performed on the equations derived in this paper. It would be of great interest to use the two-dimensional shock propagation theory of Section 6.2 to examine the stability of the plane shock waves found in Section 4.2 to spanwise disturbances. The analyses of Troian *et al.* [25] and of Bertozzi and Brenner [31] for gravity-driven flow on a flat substrate, suggest that the shocks may be susceptible to a fingering instability, at least in the limit where the film thickness ahead of the shock tends to zero. Kalliadasis and Homsy [32], however, included substrate topography and found that the corresponding capillary ridge was surprisingly stable.

Furthermore, it remains to perform a local analysis at a saddle point of the substrate curvature, as carried out in Section 6.3 for a maximum. At such a point, Λ_1 and Λ_2 take different signs, but the outer solution still predicts blow-up so long as $\Lambda_1 + \Lambda_2 > 0$. Such an analysis is complicated by the fact that the ‘puddle’ is no longer bounded, and because real solutions of (97, 98) in the form (99) do not, in general, exist.

Acknowledgements

I would like to thank Dr J.R. Ockendon for his helpful advice in the preparation of this paper and Professors O.E. Jensen and J.R. King for some informative discussions. Part of this work was carried out while the author was a Postdoctoral Research Fellow with Professor J.B. Grotberg, Biomedical Engineering Department, Northwestern University, supported by NASA grant NAG3-1636 and NSF grant CTS-9412523.

Appendix A. Arbitrary substrate motion

In general we cannot assume that our coordinate system, which is chosen to parametrise lines of curvature of the substrate surface for all time, remains fixed in the evolving substrate. The integrated conservation-of-mass equation (11) applies in any case, since its derivation relies only on continuity of normal velocity. However, the nondimensionalisation *ansatz* (7) must be modified to

$$\mu_i = \frac{\sigma L}{\mu a}\left(\mathrm{Ca}\frac{a}{L}\mathcal{U}_i + \epsilon^2 \tilde{u}_i'\right), \quad i = 1, 2, \tag{A1}$$

where $\mathcal{U}_i$ is the substrate velocity, made dimensionless with U.

With this new definition of $\tilde{u}$, the Stokes equations and boundary conditions (14–19) are preserved. Hence the flux components, scaled with $\epsilon\sigma L^2/\mu a$ are found to be

$$Q_1 = \mathrm{Ca}\frac{a}{L}(\mathcal{U}_1 - v_1)a_2\left(h - \frac{\epsilon L}{a}\frac{\kappa h^2}{2}\right) - \epsilon^2\frac{a_2}{a_1}\frac{\partial p}{\partial x_1}\frac{h^3}{3} + O\left(\epsilon^4, \frac{\epsilon^3 L}{a}, \epsilon^2\,\mathrm{Ca}\frac{a}{L}\right), \tag{A2a}$$

$$Q_2 = \mathrm{Ca}\frac{a}{L}(\mathcal{U}_2 - v_2)a_1\left(h - \frac{\epsilon L}{a}\frac{\kappa h^2}{2}\right) - \epsilon^2\frac{a_1}{a_2}\frac{\partial p}{\partial x_2}\frac{h^3}{3} + O\left(\epsilon^4, \frac{\epsilon^3 L}{a}, \epsilon^2\,\mathrm{Ca}\frac{a}{L}\right). \tag{A2b}$$

Now we transform to coordinates $(\xi_1, \xi_2; \tau)$ that are fixed in the substrate. Put

$$\boldsymbol{r}_c(x_1, x_2; t) \equiv \boldsymbol{\rho}_c(\xi_1, \xi_2; \tau). \tag{A3}$$

Using the chain rule, we see that

$$\frac{\partial \boldsymbol{\rho}_c}{\partial \tau} = \mathcal{U}_1\boldsymbol{e}_1 + \mathcal{U}_2\boldsymbol{e}_2 + v_3\boldsymbol{n} = \left(v_1 + a_1\frac{\partial x_1}{\partial \tau}\right)\boldsymbol{e}_1 + \left(v_2 + a_2\frac{\partial x_2}{\partial \tau}\right)\boldsymbol{e}_2 + v_3\boldsymbol{n},$$

i.e.,

$$\frac{\partial x_1}{\partial \tau} = \frac{\mathcal{U}_1 - v_1}{a_1}, \quad \frac{\partial x_2}{\partial \tau} = \frac{\mathcal{U}_1 - v_2}{a_2}. \tag{A4}$$

Also,

$$a_1 a_2 = \frac{\partial(\xi_1, \xi_2)}{\partial(x_1, x_2)} J, \tag{A5}$$

where

$$J\,\mathrm{d}\xi_1\mathrm{d}\xi_2 = \left|\frac{\partial \boldsymbol{\rho}_c}{\partial \xi_1} \wedge \frac{\partial \boldsymbol{\rho}_c}{\partial \xi_2}\right| \mathrm{d}\xi_1\mathrm{d}\xi_2, \tag{A6}$$

is the element of area in the new coordinate system.

Combining (A4) and (A5), we obtain the transport theorem relating the two frames:

$$\frac{1}{J}\frac{\partial}{\partial \tau}(J\Phi) = \frac{1}{a_1 a_2}\frac{\partial}{\partial t}(a_1 a_2 \Phi) + \nabla_s \cdot \left[\Phi\begin{pmatrix}\mathcal{U}_1 - v_1\\ \mathcal{U}_2 - v_2\end{pmatrix}\right]. \tag{A7}$$

Using this identity to transform (11) to the new frame, we find that the invariant form suggested by (22) is correct for arbitrary substrate motions:

$$\frac{1}{J}\frac{\partial}{\partial \tau}(Jh) + \nabla_s \cdot \left(\frac{h^3}{3}\nabla_s \mathcal{K}\right) = O\left(\epsilon^2, \frac{\epsilon L}{a}, \mathrm{Ca}\frac{a}{L}\right). \tag{A8}$$

Here, recall that the time-derivative must be taken in a frame fixed in the moving substrate.

Notes

[1] I am grateful to Professor John King for pointing this out.
[2] Bearing in mind that asymptotic series do not, in general, converge, it is more often the case that fewer terms can safely be included in an asymptotic expansion as a point of nonuniformity is approached.

References

1. L. D. Landau and V. G. Levich, Dragging of a liquid by a moving plate. *Acta Physicochim. URSS* 17 (1942) 42–54.
2. S. D. R. Wilson, The drag-out problem in film coating theory. *J. Engng. Math.* 16 (1982) 209–221.
3. W. S. Overdiep, The levelling of paints. *Prog. Org. Coat.* 14 (1986) 159–175.
4. H. Wong, I. Fatt and C. J. Radke, Deposition and thinning of the human tear film. *J. Colloid Interface Sci.* 184 (1996) 44–51.
5. D. Halpern and J. B. Grotberg, Fluid-elastic instabilities of liquid-lined flexible tubes. *J. Fluid Mech.* 244 (1992) 615–632.
6. A. Oron, S. H. Davis and S. G. Bankoff, Long-scale evolution of thin liquid films. *Rev. Modern Phys.* 69 (1997) 931–980.

7. T. G. Myers, Thin films with high surface tension. *SIAM Rev.* 40 (1998) 441–462.
8. L. E. Stillwagon and R. G. Larson, Fundamentals of topographic substrate levelling. *J. Appl. Phys.* 63 (1988) 5251–5258.
9. L. E. Stillwagon and R. G. Larson, Leveling of thin films over uneven substrates during spin coating. *Phys. Fluids A* 2 (1990) 1937–1944.
10. S. Kalliadasis, C. Bielarz and G. M. Homsy, Steady free-surface thin film flows over topography. *Phys. Fluids* 12 (2000) 1889–1898.
11. A. Mazouchi and G. M. Homsy, Free surface Stokes flow over topography. *Phys. Fluids* 13 (2001) 2751–2761.
12. L. W. Schwartz and D. E. Weidner, Modelling of coating flows on curved surfaces. *J. Engng. Math.* 29 (1995) 91–103.
13. M. Hayes, S. B. G. O'Brien and J. H. Lammers, Green's function for steady flow over a small two-dimensional topography. *Phys. Fluids* 12 (2000) 2845–2858.
14. F. P. Bretherton, The motion of long bubbles in tubes. *J. Fluid Mech.* 10 (1961) 166–188.
15. P. S. Hammond, Nonlinear adjustment of a thin annular film of viscous fluid surrounding a thread of another within a circular pipe. *J. Fluid Mech.* 137 (1983) 363–384.
16. R. W. Atherton and G. M. Homsy, On the derivation of evolution equations for interfacial waves. *Chem. Engng. Comm.* 2 (1976) 57–77.
17. M. Cheng and H.-C. Chang, Stability of axisymmetric waves on liquid films flowing down a vertical column to azimuthal and streamwise disturbance. *Chem. Engng. Comm.* 118 (1992) 327–334.
18. A. L. Frenkel, On evolution equations for thin films flowing down solid surfaces. *Phys. Fluids A* 5 (1993) 2342–2347.
19. B. Reisfeld and S. G. Bankoff, Non-isothermal flow of a liquid film on a horizontal cylinder. *J. Fluid Mech.* 236 (1992) 167–196.
20. P. A. Gauglitz and C. J. Radke, The dynamics of liquid film breakup in constricted cylindrical capillaries. *J. Colloid Interface Sci.* 134 (1990) 14–40.
21. O. E. Jensen, The thin liquid lining of a weakly curved cylindrical tube. *J. Fluid Mech.* 331 (1997) 373–403.
22. Lord Rayleigh, On the instability of jets. *Proc. London Math. Soc.* **10** (1878) 4–13.
23. R. V. Roy, A. J. Roberts and M. E. Simpson, A lubrication model of coating flows over a curved substrate in space. *J. Fluid Mech.* 454 (2002) 235–261.
24. H. E. Huppert, Flow and instability of a viscous current down a slope. *Nature* 300 (1982) 427–429.
25. S. M. Troian, E. Herbolzheimer, S. A. Safran and J. F. Joanny, Fingering instabilities of driven spreading films. *Euro. Phys. Lett.* 10 (1989) 25–30.
26. J. A. Moriarty, L. W. Schwartz and E. O. Tuck, Unsteady spreading of thin liquid films with small surface tension. *Phys. Fluids A* 3 (1991) 733–742.
27. B. W. van de Fliert, P. D. Howell and J. R. Ockendon, Pressure-driven flow of a thin viscous sheet. *J. Fluid Mech.* 292 (1995) 359–376.
28. P. D. Howell, S. L. Waters and J. B. Grotberg, The propagation of a liquid bolus along a liquid-lined flexible tube. *J. Fluid Mech.* 406 (2000) 309–335.
29. E. Kreyszig, *Differential Geometry*. New York: Dover (1991) 352pp.
30. S. D. R. Wilson and A. F. Jones, The entry of a falling film into a pool and the air-entrainment problem. *J. Fluid Mech.* 128 (1983) 219–230.
31. A. L. Bertozzi and M. P. Brenner, Linear stability and transient growth in driven contact lines. *Phys. Fluids* 9 (1997) 530–539.
32. S. Kalliadasis and G. M. Homsy, Stability of free-surface thin-film flows over topography. *J. Fluid Mech.* 448 (2001) 387–410.